Top Curr Chem (2007) 272: 51–82
DOI 10.1007/128_2006_090

Published online: 20 October 2006

Dynamics and Thermodynamics of Ligand–Protein Interactions

S. W. Homans

Astbury Centre for Structural Molecular Biology, University of Leeds, Leeds LS2 9JT, UK
s.w.homans@leeds.ac.uk

Abstract Protein–ligand interactions are of fundamental importance in a great many biological processes. However, despite enormous advances in the speed and accuracy of the three-dimensional structure determination of proteins and their complexes, our ability to predict binding affinity from structure remains severely limited. One reason for this dilemma is that affinities are governed not only by energetic considerations arising from the precise spatial disposition of interacting groups (loosely, enthalpy), but also by the dynamics of these groups (loosely, entropy) including solvent effects. In this work I will review current methodology for unravelling this complex problem, including X-ray crystallography, NMR, isothermal titration calorimetry and theoretical free energy perturbation methods.

Keywords ITC · Ligand · NMR · Protein · Solvation · Thermodynamics

1 Introduction

1.1 Biomolecular Interactions

Biomolecular interactions are of fundamental importance in biological processes. However, despite enormous advances in the speed and accuracy of the three-dimensional structure determination of proteins and their complexes, our ability to predict binding affinity from structure (i.e. whether and how strongly two molecules will interact) remains severely limited. One reason for this dilemma is that affinities are governed not only by energetic considerations arising from the precise spatial disposition of interacting groups (loosely, enthalpy), but also by the dynamics of these groups (loosely, entropy). Thus, in order to predict accurately the affinity of a protein for a given ligand, it is essential to have knowledge of both of these factors. While arguably it is possible to obtain a good estimate of the enthalpy of binding on a per-residue basis from a high-resolution crystal structure of the complex together with molecular mechanical energy calculations, it is not possible to obtain the entropy from this static model. Moreover, a simple static picture provides no information on the role of solvent reorganization to the binding affinity, the importance of which is still a subject of much debate. The following pages describe recent experimental and theoretical developments aimed at understanding the various individual contributions to the overall free energy of binding.

2 Thermodynamic Principles

2.1 Free Energy, Enthalpy and Entropy

Enthalpy and entropy are encompassed in the fundamental thermodynamic equation that describes the Gibbs free energy of binding, ΔG_b:

$$\Delta G_b = \Delta H_b - T\Delta S_b \,, \tag{1}$$

where ΔH_b and ΔS_b represent the enthalpy and entropy of binding, respectively, and T is the absolute temperature. In any spontaneous process the free energy is minimized, hence a negative ΔG implies that a reaction or process will proceed in the direction as written. Thus, a ligand L will only associate with a protein P if ΔG_b for the following process is negative:

$$P + L \rightarrow PL \,. \tag{2}$$

Thermodynamic arguments enable us to determine the strength of binding via the affinity (association constant) K_a by use of a second fundamental relationship:

$$\Delta G_b^o = - RT \ln K_a \, . \tag{3}$$

The term on the left-hand-side of Eq. 3 is the *standard* Gibbs free energy of binding, which is the free energy of binding measured under certain defined standard conditions. This term is often confused with the free energy of binding. This confusion is not based upon semantics, since in general these two terms will differ numerically. This can be understood with reference to Eq. 4, which directly relates the free energy of binding and the standard free energy of binding:

$$\Delta G - \Delta G_b^o = RT \ln Q \, . \tag{4}$$

Here, Q is the reaction quotient, which is expressed in terms of the concentrations of products and reactants. Thus, for the process shown in Eq. 2:

$$Q = [PL] \, / \, [P] \, [L] \, . \tag{5}$$

At equilibrium, Q is equivalent to the equilibrium constant for the process, which in turn is equivalent to the affinity K_a, and since ΔG is zero at equilibrium, Eq. 3 follows directly from Eq. 4. Thus, while ΔG is zero at equilibrium, ΔG_b^o in general is not, except in the case that $K_a = 1$.

It is important to appreciate the molecular interpretation of Eqs. 3 and 4, which lies in the concept of the entropy of mixing. Consider a hypothetical case in which species A that exists in a specified standard state is converted to B, also in the standard state, such that there is no mixing of A and B. The change in free energy with respect to the mole fraction of B is described by the dotted line in the upper panel of Fig. 1. However, in all practical cases there will be a mixing of reactants and products, resulting in an increase of the entropy of the system. The Gibbs free energy of mixing is:

$$\Delta G = RT \left[x_a \ln x_a + x_b \ln x_b \right] \, , \tag{6}$$

where x_a and x_b are the mole fractions of A and B. This function is plotted in the lower panel of Fig. 1 for a process at 300 K. The free energy of the system will consist of one part derived from the free energy of the pure components multiplied by their mole fractions, and a second part derived from the free energy of mixing. Thus,

$$\Delta G = x_b \Delta G^o + RT \left[\left(1 - x_b\right) \ln \left(1 - x_b\right) + x_b \ln x_b \right] \, . \tag{7}$$

This function is represented by the solid line in the upper panel of Fig. 1.

At equilibrium, the free energy is zero, i.e. when the slope of the solid line in the upper panel of Fig. 1 is zero:

$$d\Delta G / dx_b = \Delta G^o + RT \left[- \ln \left(1 - x_b\right) + \ln x_b \right] = 0 \, , \tag{8}$$

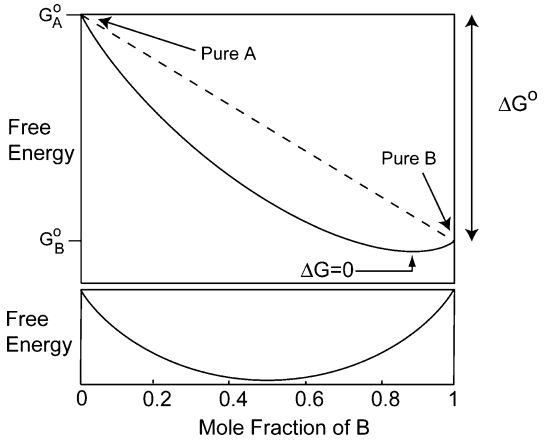

Fig. 1 Standard free energy changes in the conversion of species A to species B. In the hypothetical case that A is converted to B without mixing of the two components, the change in the standard free energy of binding will be linear with respect to the mole fraction of B, and is described by the *dashed line*. However, in any practical case there will be a mixing of A and B as A converts to B. A change in free energy is associated with this process resulting from the entropy of mixing (represented by the *solid line* in the *lower panel*), which is minimal at equal mole fractions of A and B, i.e. where the entropy of mixing is maximal. The observed free energy change is given by the *solid line* in the *upper panel* and equals the sum of the standard free energy change and the contribution from mixing. At equilibrium $\Delta G = 0$, i.e. where the slope of the free energy curve is at a minimum

which is equivalent to Eq. 3:

$$\Delta G^{\mathrm{o}} = -RT \ln \left(x_{\mathrm{b}}^{\mathrm{eq}} / \left(1 - x_{\mathrm{b}}^{\mathrm{eq}}\right) \right) = -RT \ln K \,, \tag{9}$$

where $x_{\mathrm{b}}^{\mathrm{eq}}$ is the mole fraction of B at equilibrium and K is the equilibrium constant for the process. Thus, the free energy change for a given process can be thought of as comprising the standard free energy change plus a term related to the entropy of mixing. The position of equilibrium for processes with a large negative standard free energy change will lie towards products, whereas processes with a large positive standard free energy will lie towards reactants.

2.2 The Hydrophobic Interaction and Heat Capacity

The hydrophobic interaction arises from the low solubility of nonpolar compounds in water. At physiological temperature the driving force derives from the unfavourable decrease in entropy of the hydrating waters. Water molecules are unable to hydrogen-bond to nonpolar solutes, resulting

in a disruption of the favourable hydrogen-bonding network of bulk water. Those water molecules that are in contact with the solute compensate by bonding more strongly to their neighbours, resulting in an ordering of water molecules around the solute. This ordering has variously been described as "clathrate-type", "icelike", icebergs and flickering clusters [1–3]. The minimization of exposed surface area of solute results in a release into bulk solvent of a proportion of these ordered water molecules (Fig. 2). This is an entropically favourable process which therefore results in the burial of nonpolar surface area from water. A further consequence of this process is that the number of water–water contacts increases and more water–water hydrogen bonds can form. Thus, it might be anticipated that the hydrophobic interaction would be accompanied by a decrease in enthalpy. However, at physiological temperatures, the stronger bonding of water molecules in clathrate structures surrounding the nonpolar solute compensates for the smaller number of hydrogen bonds that can be formed, and the net enthalpy change is close to zero. Despite this interpretation, many "hydrophobic interactions" possess an enthalpy-driven thermodynamic signature, for subtle reasons that will be discussed in Sect. 3.2.1. Although we are only concerned below with thermodynamic processes occurring at physiological temperature, it is worth noting that at higher temperatures the hydrophobic effect becomes enthalpy driven, to the point where the entropy of nonpolar surface burial is approximately zero [4].

Large changes in heat capacity (C_p) are often taken as evidence for the existence of the hydrophobic interaction in biomolecular recognition. This interpretation derives from data for the transfer of hydrophobic solutes from nonaqueous to aqueous environments, which is generally accompanied by a positive ΔC_p. A simple molecular interpretation of this phenomenon is that the progressive "melting" of hydrogen-bonded water structure around

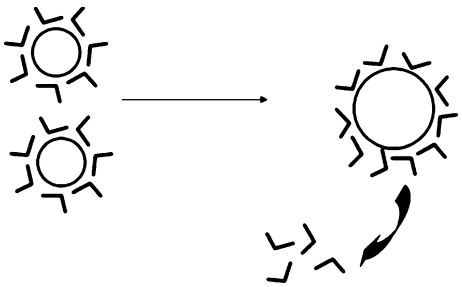

Fig. 2 "Clathrate" model of the hydrophobic effect. Water molecules that are in contact with the hydrophobic solute compensate by bonding more strongly to their neighbours, resulting in an ordering of water molecules around the solute. Minimization of exposed surface area of the solute is proposed to result in a release into bulk solvent of a proportion of these ordered water molecules. This is an entropically favourable process that therefore derives the association of hydrophobic species at physiological temperature

nonpolar solutes as the temperature is increased "absorbs" the increase in thermal energy, thus resulting in increased heat capacity. Arnett and co-workers were the first to demonstrate that the heat capacity increment for the dissolution of nonpolar solutes is a unique property of water, and is not observed in any other solvent [5]. In the case of protein-protein and ligand-protein interactions, the burial of hydrophobic surface area conversely gives rise to a significant negative ΔC_p, which is thus taken as a further thermodynamic signature of the hydrophobic effect.

It is important to note that the above view of the hydrophobic effect, while predominant, is not universally accepted. Indeed, despite much effort, there is little physical evidence for the existence of water clathrates surrounding nonpolar solutes. The "Small-Size Model" [6–9] has been proposed as an alternative to the "iceberg" model. This model is concerned with free energies of solvation (Sect. 3.2.2) rather than entropy and heat capacity. The high free energy cost of incorporation of a nonpolar solute into water is argued to arise from the absence of an appropriate cavity in water due to its small size. Large cavities are more likely in solvents comprised of large molecules, and since water molecules are amongst the smallest solvent molecules, the free energy cost of creating a cavity is greater in water than other solvents. In general the creation of a cavity by the coalescence of a number of smaller volumes throughout the solvent will lead to an entropic cost, together with an enthalpic cost of breaking solute–solute intermolecular interactions. In the "special" case of solvent water, the Small-Size Model suggests that the additional entropic cost of ordering waters in the solvation shell and the favourable enthalpic contribution due to stronger hydrogen bonding in this shell compensate almost perfectly (i.e. enthalpy-entropy compensation), and thus does not contribute to the free energy of cavity formation [7]. However, using the so-called "MB" model of water, Dill and co-workers [10, 11] showed that such compensation is limited to small nonpolar solutes, and suggested that "water's complexities appear to be important in most other circumstances".

More recent theoretical treatments further support the view that hydrophobicity manifests different characteristics depending on whether small molecular units or large clusters are involved, either alone or in combination [12]. In the small molecule case (such as methane), a cavity is created in the solvent that excludes water molecules from a spherical volume less than 0.5 nm in diameter. This volume is sufficiently small to permit hydrogen-bonding patterns to go around the solute, and thus the extent to which hydrogen bonds are broken at any given time is similar to that in pure water. However, in larger complexes, where the solute surface extends over areas larger than 1 nm^2, it is impossible for adjacent water molecules to maintain a complete hydrogen-bonding network. As a result, water tends to move away from the large solute and forms an interface that bears a similarity to that between a vapour and a liquid. This phenomenon provides a physical basis for

the understanding of hydrophobic effects in that statistical thermodynamical calculations on the formation of small cavities in water accurately reproduce the entropy and heat capacity of solvation of, for example, methane. Moreover, the driving force for hydrophobic association is readily understood in terms of the dependence of hydrophobic solvation on solute size—when solute molecules cluster to form a hydrophobic complex, the overall solvation energy can be shown to change from a linear dependence on solvent volume to a linear dependence on solvated surface area. Thus, if the number of solute molecules in the cluster is sufficiently large, the volume to surface area ratio will result in a solvation free energy that is lower than the solvation free energy of the individual components. This results in a favourable driving force for association. A compelling advantage of this model is that it can be observed in simulations, unlike the "clathrate" model.

3
Dynamics and Thermodynamics of Biomolecular Associations

3.1
Overview of the Binding Process

Before embarking on a detailed analysis of the factors responsible for biomolecular interactions, it is worthwhile initially to examine the qualitative aspects of the process. The interaction between a protein and a ligand is often described schematically by Eq. 2. However, this is a gross over-simplification for two reasons.

First, Eq. 2 does not describe all of the partners in the interaction. Since we are concerned with biomolecular interactions, all such processes take place within an aqueous *milieu*. The individual species will thus interact with solvent water in some manner before the association. For example, as discussed in Sect. 2.2, hydrophobic ligands will be surrounded by icelike cages of water molecules or water-vapour interfaces (provided they are of sufficient size), and binding pockets within proteins will also typically contain solvent water molecules that may be ordered to some degree. When the two species associate, their interaction with solvent will certainly be entirely different. For example, some or all of the solvent water molecules within the binding pocket are likely to be expelled as the ligand binds. Moreover, the expelled solvent molecules will make new interactions with bulk solvent. Since the free energy of binding is defined as the difference between the free energy of the system (solutes plus solvent) in the complexed state versus the uncomplexed state, it follows that solvent reorganization can have a dramatic influence on binding.

Second, Eq. 2 assumes that the structures of the interacting species before and after association will be equivalent. However, it is very likely that structural changes will occur following complexation, and hence formally we are

dealing with different species before and after complexation, in which case Eq. 2 should more formally be written [13]:

$$P + L \rightarrow P'L' \,. \tag{10}$$

It is important to be aware that the contribution of solvation or structural changes to binding affinity can be dramatic. A simple calculation using Eq. 3 shows that the difference between micromolar and nonamolar affinity results from a change in free energy at 300 K of ~ 17 kJ/mol, which is on the order of the strength of a hydrogen bond. Thus, the loss of an ordered water molecule from a protein binding pocket or the reorientation of an amino-acid residue side-chain may be sufficient to alter binding affinity by orders of magnitude. It follows that a quantitative description of the thermodynamics of ligand-protein association requires full account to be taken of all interacting species at every stage of the process. A convenient formalism involves the use of Born–Haber cycles.

3.1.1 Born–Haber Cycles

The representation of ligand-protein association in the form of a Born–Haber cycle offers a rigorous conceptual framework which includes all the interacting species. A typical cycle is shown in Fig. 3. The "intrinsic" standard free energy of binding between protein P and ligand L is represented by ΔG_i°, whereas the standard free energy of binding that would typically be determined experimentally is represented by $\Delta G_{\text{obs}}^{\circ}$. In addition, two further processes can be defined which are represented by $\Delta G_{\text{su}}^{\circ}$ and $\Delta G_{\text{sb}}^{\circ}$. These are the standard free energies of solvation of the uncomplexed species and the complex, respectively. Since free energy is a state function, it is independent of the path taken from one state of the system to another, and we can therefore write:

$$\Delta G_i^{\circ} + \Delta G_{\text{sb}}^{\circ} = \Delta G_{\text{su}}^{\circ} + \Delta G_{\text{obs}}^{\circ} \,, \tag{11}$$

which can be rearranged:

$$\Delta G_{\text{obs}}^{\circ} = \Delta G_i^{\circ} + \left\{ \Delta G_{\text{sb}}^{\circ} - \Delta G_{\text{su}}^{\circ} \right\} \,. \tag{12}$$

Equation 12 shows how the observed standard free energy of binding can be decomposed into the intrinsic contribution plus a solvation term shown in curly braces. Equivalent expressions can be written for the standard enthalpy and standard entropy of binding since these parameters are also state functions.

The advent of sensitive isothermal titration calorimetry [14] has enabled the accurate determination of $\Delta G_{\text{obs}}^{\circ}$, $\Delta H_{\text{obs}}^{\circ}$ and $\Delta S_{\text{obs}}^{\circ}$ for a wide variety of biomolecular complexes in aqueous solution. However, this technique measures the global thermodynamics of binding including solvation effects, as

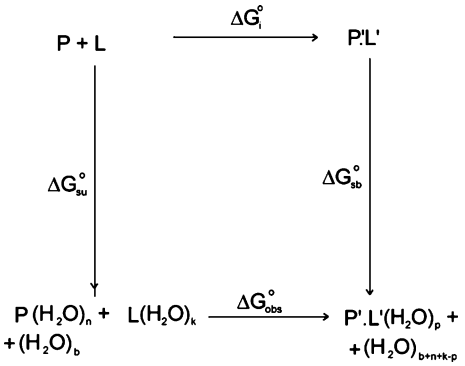

Fig. 3 A typical Born–Haber cycle relating the "intrinsic" (solute-solute) standard free energy of binding $\Delta G_{\mathrm{i}}^{\mathrm{o}}$ with the observed standard free energy of binding $\Delta G_{\mathrm{obs}}^{\mathrm{o}}$ for a protein *P* interacting with a ligand *L*. The vertical processes represent the solvation free energies of the uncomplexed species $\left(\Delta G_{\mathrm{su}}^{\mathrm{o}}\right)$ and of the complex $\left(\Delta G_{\mathrm{sb}}^{\mathrm{o}}\right)$

defined in Eq. 12. In many cases it is therefore practically impossible to delineate the factors responsible for the association process. The key to a complete quantitative understanding of the thermodynamics of ligand-protein association requires a deconvolution of the overall thermodynamics of binding into the terms on the right-hand side of Eq. 12. For this purpose it is convenient to consider the enthalpic and entropic contributions separately, as detailed below.

3.2 Enthalpic Contributions to Binding

3.2.1 Intrinsic Contributions to Binding Enthalpy

Intrinsic contributions to binding enthalpy result from differences in nonbonded interactions within each species prior to complexation versus those present in the complex. (Strictly, we should also include covalent interactions, since complexes exist involving the formation of solute–solute covalent bonds, but we will not consider such systems here). Thus, the intrinsic standard enthalpy of binding ΔH_i^{o} can be thought of as the total change in internal energy of the interacting species in vacuo.

If we first consider the uncomplexed ligand, this will exist in one or more conformations whose populations are governed by the Boltzmann distribution at a given temperature. The internal energies of these conformers will depend upon a complex interplay between dispersive interactions, Coulombic interactions and hydrogen bonding. On binding to the protein receptor, typically only one of these conformations will be selected, or indeed none if

there is conformational strain on binding. In general, the result will be an unfavourable contribution to binding enthalpy. The size of this unfavourable contribution will obviously depend upon the nature of the ligand. As examples, methyl-methyl gauche interactions represent approximately 1 kJ/mol of unfavourable enthalpy, whereas the barrier to rotation about the carbon-carbon bond of ethane is approximately 12 kJ/mol. Thus, even small deviations from minimum energy conformations can result in significant unfavourable contributions to the binding free energy.

Similar considerations exist for the protein receptor. Penel and Doig have quantified strain energies for amino-acid residues in α-helices in the context of protein folding [15]. The mean change in rotameric strain energy (i.e. the energy resulting from a side-chain that is not in its lowest-energy rotamer) was 1.75 kJ/mol, whereas the mean dihedral strain energy (i.e. the energy resulting from a shift of a dihedral angle from the most stable conformation of a rotamer) was reported as 2.67 kJ/mol. It is anticipated that unfavourable enthalpic contributions of this magnitude will exist in the context of ligand-protein interactions also, and this contribution may be very significant due to the many additional degrees of freedom within a typical protein binding site.

Paradoxically, evidence exists that the many degrees of freedom and resulting interactions within the protein structure can in principle result in improved ligand binding as a result of "tightening" of the protein structure on association. Williams and co-workers have obtained experimental support for this hypothesis in, for example, the binding of biotin to the streptavidin tetramer [16]. The binding of these species is about 1000-fold stronger than anticipated on the basis of the sum of the individual interactions. Williams and co-workers used mass spectrometry to measure the extent of hydrogen/deuterium exchange of the amide protons in streptavidin in the absence and presence of biotin. Twenty-two amide protons per streptavidin monomer were found to be protected upon binding of biotin. The latter reduced the solvent accessibility in much of the structure, indicating a global tightening of the structure rather than a localized effect at the ligand-protein interface. This phenomenon is further emphasized in the thermal stability of streptavidin evaluated using differential scanning calorimetry [17]—biotin binding increases the thermal denaturation of streptavidin from T_m = 75 °C to 112 °C, indicating that the complex is more stable than the uncomplexed protein. These data support positively cooperative binding whereby the ligand reduces the dynamic behaviour of the receptor. Williams has proposed [16] that this does not necessarily involve the formation of new noncovalent interactions within the receptor, rather tightening of existing interactions. Major conformational changes need not thus be invoked. The generality of this phenomenon remains to be determined, but examples certainly exist where this phenomenon is not the driving force for association (see below).

In addition to the modification of nonbonded interactions that pre-exist in the protein and ligand prior to association, nonbonded interactions form

at the solute–solute interface. Naively, it might be thought that each of these "new" interactions will contribute favourably to the enthalpy of binding. For example, ab initio quantum chemical calculations suggest stabilization of the core of the small protein rubredoxin resulting from dispersion interactions by approximately – 200 kJ/mol [18]. Correspondingly, large intrinsic stabilization enthalpies are expected in ligand-protein complexes. However, it must be remembered that prior to the association each binding partner will form dispersive interactions with solvent water. Indeed, it is commonplace to assume that the change in dispersion energy on association of two shape complementary molecules in solution is negligible, since new solute–solute dispersion interactions following association have "exchanged" for solute–solvent dispersion interactions that exist prior to the association (Fig. 4). However, recent evidence suggests that this assumption may not generally be true for some ligand-protein associations. Very recently, Barratt et al. examined the binding thermodynamics of the mouse major urinary protein (MUP), a promiscuous binder of small hydrophobic ligands (see Sect. 4). Despite the fact that the binding site is extremely hydrophobic, the association with a variety of different hydrophobic ligands is invariably strongly enthalpy driven. This is counter-intuitive, based upon the expected thermodynamic signature of the hydrophobic effect [19]. However, detailed scrutiny of the binding pocket of this protein by site-directed mutagenesis, X-ray crystallography and molecular dynamics simulations, revealed that the binding pocket is poorly solvated in the absence of ligand. Thus, in this particular system the gain in solute–solute dispersion energy will not be compensated by interactions between binding-site residues and solvent prior to the association. A significant fraction of the favourable intrinsic solute–solute enthalpy is thus expected to appear in the free energy of binding, which thus accounts for an enthalpy-driven thermodynamic signature. This conclusion is indeed supported by molecular mechanical energy calculations, and is reminiscent of the interaction of small organic molecules in nonaqueous solvents where the geometry of the binding pocket prevents solvation [20, 21].

It must be emphasized that these observations are not necessarily at variance with current models of the hydrophobic effect. Rather, they may offer an explanation for the fact that many "hydrophobic associations" in solution do not possess the anticipated entropy driven thermodynamic signature—many,

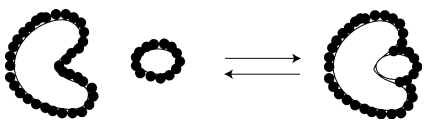

Fig. 4 Prior to association, both ligand and protein partake in dispersive interactions with solvent molecules. Following association, it is generally assumed that these solute–solute dispersive interactions exchange for solute–solute dispersive interaction, with a negligible net contribution to the binding enthalpy

but by no means all. For example, the binding of a series of hydrophobically modified benzamidinium chloride inhibitors to trypsin is strongly entropy driven at a number of temperatures [22]. Notably, the trypsin binding site is a cleft that is presumably heavily solvated. These data are thus consistent with a model whereby the degree of expression of the intrinsic solute–solute enthalpic contribution to the free energy of binding is dependent on the solvation of the protein binding pocket.

In addition to dispersive interactions, it might be anticipated that the formation of hydrogen bonds at the solute–solute interface will result in a favourable contribution to the enthalpy of binding. However, again it must be remembered that the relevant hydrogen bond donors and acceptors will interact with solvent water molecules prior to the association. Nonetheless, evidence exists that solute–solute hydrogen bonds are stronger than solute–solvent hydrogen bonds, giving rise to a nett favourable enthalpy of binding. Daranas et al. [23] determined the global thermodynamics of binding of galactose and various deoxy derivatives to the arabinose binding protein (Table 1). Binding of all ligands was found to be enthalpy driven, and with the exception of charged ligands such as heparin and heparin sulphate, both ΔH^{o} and particularly $T\Delta S^{o}$ are significantly larger than typical values reported for the vast majority of carbohydrate-protein interactions [24], including oligosaccharides. The reason for these anomalously large values could not be delineated with certainty from global thermodynamics measurements. However, the enthalpy of binding of galactose compared with 1-deoxy, 2-deoxy or 3-deoxy galactose was found to be favourable by ~ 30 kJ/mol. As mentioned above, it might be considered unlikely that the more favourable enthalpy of binding of galactose compared with deoxy-derivatives arises from the additional hydrogen bond(s) that form due to the additional hydroxyl group in the complex, since prior to binding, the ligand is hydrogen bonded to solvent water. The enthalpic component of such solute–solvent hydrogen bonds is contained within the free energy of solvation of these ligands, which is not known with any degree of accuracy. However, intuitively, the solvation enthalpy of deoxy-analogues of galactose must be less favourable than those of

Table 1 Thermodynamics of binding of galactose and derivatives to the arabinose-binding protein derived from ITC measurements at 308 K

Ligand	K_d (μM)	Error μM	ΔG^{o} (kJ/mol)	Error	ΔH^{o} (kJ/mol)	Error	$T\Delta S^{o}$ (kJ/mol)	Error
galactose	2.2	0.02	– 33.36	0.3	– 95	0.6	– 61	0.6
1-deoxy	14 600	730	– 10.8	0.5	– 63	3	– 52	3
2-deoxy	780	60	– 18.3	1.4	– 61	4.8	– 43	4.8
3-deoxy	29 620	2620	– 9.0	0.8	– 57	5	– 48	5

galactose. If one assumes momentarily that the enthalpic contribution from ligand-protein hydrogen bonds is effectively zero, since hydrogen bonds to solvent exist prior to the association, on the basis of the above data one must conclude that the enthalpies of solvation of the 1-deoxy, 2-deoxy and 3-deoxy analogues of galactose are each more favourable than galactose by ~ -30 kJ/mol, which is counter-intuitive. Therefore, the conclusion that interactions between the various hydroxyl groups of galactose and the protein are enthalpically significantly more favourable than those with solvent would appear to be inescapable. Whether this favourable enthalpy can be attributed in the main to hydrogen bonding is difficult to ascertain, since the loss of an hydroxyl group removes van der Waals' interactions with that group in addition to the hydrogen bonding contribution.

3.2.2
Solvation Contribution to Binding Enthalpy

The solvation contribution to binding enthalpy, $\left\{\Delta H^{o}_{sb} - \Delta H^{o}_{su}\right\}$, is essentially comprised of the enthalpy of solvation of the complex minus the enthalpy of solvation of species prior to the association. The enthalpy of solvation of any species is defined as the heat gained or lost when that species is transferred from the gas phase into solution. When the solvent is water this parameter is sometimes called the enthalpy of hydration. This definition may appear to be somewhat abstract or esoteric in the context of ligand-protein association phenomena, but is nonetheless an integral part of the rigorous description of binding thermodynamics as is apparent from Fig. 3. In many respects, the binding process can be thought of as desolvation. Qualitatively, we can think of this as the stripping of some or all solvent water molecules from the surface of the ligand and from the protein binding pocket as the partners associate. Quantitatively, the desolvation process is represented by the negative of the solvation enthalpy term in the above expression.

The solvation enthalpies of a number of small organic molecules have been measured, and have been catalogued by Cabani et al. [25] and more recently by Plyasunov and Shock [26]. Solvation enthalpies of such molecules are invariably negative, i.e. desolvation upon association contributes unfavourably to the enthalpy of binding. That solvation is an exothermic process was originally regarded as counter-intuitive prior to current models of the hydrophobic effect—the large heat of vaporization and surface tension of water implied that the creation of a cavity to accommodate the solute would require a significant energy input. However, increased or strengthened hydrogen bond formation in the solvent surrounding nonpolar solutes would be anticipated in the models of the hydrophobic effect described in Sect. 2.2. The overall enthalpy of solvation will thus comprise a positive term associated with the formation of a cavity, which is more than compensated by a negative term associated with solvent ordering [27].

In theory, the standard free energy of solvation of any ligand is straightforward to measure, since it is necessary only to determine the concentrations of the ligand in aqueous solution and in the vapour phase in a closed system at equilibrium. The solvation free energies of volatile nonpolar compounds have been determined in this manner [28]. The standard enthalpy (and thus entropy) of solvation can then be estimated from the temperature dependence of the free energy. However, such measurements are only possible if the volatility is sufficient to offer a measurable concentration in the vapour phase. This excludes a number of biologically important ligands such as polar species or carbohydrates, for example. For these reasons there has recently been a surge of interest in the computation of solvation free energies of such molecules (reviewed by Orozco and Luque [29]).

The solvation process can conveniently be decomposed into three steps: (i) creation of a cavity in the solvent; (ii) van der Waals interactions and (iii) electrostatic contributions. The first step is clearly the creation of a cavity in the solvent that is large enough to accommodate the solute. Since this will involve breakage of the forces maintaining cohesion within the solvent, the free energy contribution to cavitation (ΔG_c) will be unfavourable. In contrast, the van der Waals contribution (ΔG_{vdW}) is favourable, since the solute cavity is created in regions of the solvent where the dispersion term is larger than the repulsion term. The third step (ΔG_{ele}) involves two components, namely the work necessary to create the gas-phase charge distribution of the solute in solution, and the work required to polarize this charge distribution by the solvent. Thus, the overall solvation free energy can be described by:

$$\Delta G^{o}_{solv} = \Delta G^{o}_{c} + \Delta G^{o}_{vdW} + \Delta G^{o}_{ele} \,. \tag{13}$$

The breakdown of the solvation process in this manner facilitates theoretical approaches to the computation of solvation free energies. Explicit solvent models provide the most complete description of solvation, but they are however extremely computationally demanding in view of the large number of atoms involved and the requirement to average over many solvent configurations. A particularly useful approach involves free energy perturbation (FEP) techniques [30], which have been shown to reproduce experimental solvation free energies of small organic molecules with impressive accuracy [31–33]. The conceptual basis for FEP calculations lies in the now familiar Born–Haber cycle (Sect. 3.1.1) for the conversion of a given ligand molecule A into a related molecule B (Fig. 5). The free energy of solvation can be defined as the difference between the free energies associated with the annihilation of a molecule in the gas phase and solution (Fig. 5a). Alternatively, the method can be used to determine the difference in solvation free energy between two related ligands (Fig. 5b). While it is difficult to compute directly the free energy difference between either ligand in the gas phase versus the aqueous phase (vertical processes in Fig. 5b), it is relatively straightforward to compute the free energy difference between molecules A and B in the gas

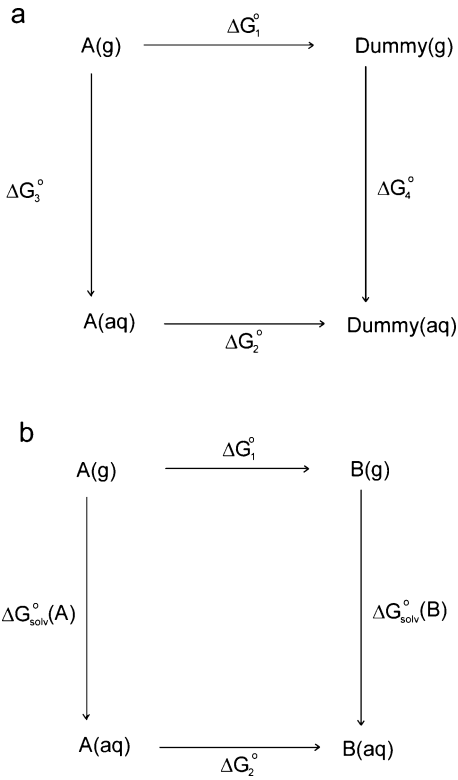

Fig. 5 The conceptual basis for FEP calculations can be described by Born–Haber cycles (Sect. 3.1.1) for the conversion of a given ligand molecule A into a related molecule B. The free energy of solvation can be defined as the difference between the free energies associated with the annihilation of a molecule in the gas phase and solution (**a**) or, alternatively, the method can be used to determine the difference in solvation free energy between two related ligands (**b**)

phase and in the solution phase (horizontal processes in Fig. 5b). Essentially, molecule A is either slowly annihilated (Fig. 5a) or "mutated" to molecule B in the gas and solution phases. In the latter case, since G is a state function, we can compute the difference in solvation free energy between two related ligands according to:

$$\Delta G^{o}_{solv}(A) - \Delta G^{o}_{solv}(B) = \Delta G^{o}_{1} - \Delta G^{o}_{2} \,. \tag{14}$$

The free energy differences ΔG^{o}_{1} and ΔG^{o}_{2} between related systems A and B represented by Hamiltonian H_A and H_B can be computed in a variety of ways. This free energy difference can be represented as:

$$\Delta G = - RT \ln \left\langle e^{-\Delta H/RT} \right\rangle_{A} \,, \tag{15}$$

where $\Delta H = H_B - H_A$ and $\langle \rangle_A$ refers to an ensemble average over a system represented by Hamiltonian H_A. If the difference between systems A and B is other than trivial, then the resulting free energy difference in Eq. 15 will not be realistic. In the FEP approach, the calculation is therefore decomposed into a number of discrete windows, each involving a very small perturbation that allows the free energy to be determined accurately. However, this is only effective if molecules A and B are structurally similar, otherwise statistical noise becomes a major problem. Provided this limitation is met, it is possible to obtain reasonably accurate values for not only the solvation free energy, but also solvation enthalpies and entropies from the temperature dependence of the free energy using, for example, finite-difference methods [34, 35]. The full details of free energy perturbation methods are outside the scope of this work, and the reader is referred to several excellent reviews on the topic [29, 30].

In contrast to small organic molecules, quantitative data for the solvation free energies of proteins and protein–ligand complexes are in general lacking. Nonetheless, it is clear from the Born–Haber cycle of Fig. 3 that this information is required for a complete understanding of the binding process. Because of the huge computational cost, it is currently not realistic to compute solvation free energies for proteins and protein–ligand complexes using explicit solvation models such as those used in FEP calculations. Implicit solvent models offer an attractive alternative. In principle, to a first approximation the free energy of solvation can be derived from the intrinsic solvation properties of the constituent groups in the molecule. This "fractional approach" has however seldom been used for the practical computation of solvation free energies. Instead, methods based on a solvent-accessible surface have commonly been employed. In the early work of Chothia [36], a general empirical solvation parameter, σ, equal to 24 cal mol^{-1} A^{-2} was derived to compute protein hydrophobicity from the solvent accessible surface area of exposed residues. The solvation free energy of the protein is thus given by:

$$\Delta G_{sol} = \sum_{k=1}^{N} \sigma_k A_k \,, \tag{16}$$

where σ_k and A_k respectively represent the solvation parameter and solvent accessible surface area of residue k.

While useful, calculations based on solvent accessible surface are subject to a number of limitations. First, the suitability of data for small molecules extrapolated to proteins is questionable. Second, screening of intrasolute interactions by the solvent is ignored. Third, recent work suggests that a particular parametrization of the surface-area model is only applicable to a subset of the conformations of the molecule included in the parametrization [37]. Finally, and perhaps most importantly, electrostatic contributions to solvation are ignored. The intrinsic solvation properties of a given atom depend upon neighbours, whose effects can be included explicitly by considering

their electrostatic contribution to solvation. Many empirical methods account for this contribution implicitly by defining different parameters according to the nature of neighboring groups. A promising, more complex strategy has been developed by Hawkins et al. [38], where atomic solvation parameters for each atom in a molecule are parameterized depending on their environment. The method reproduces the solvation free energies of small organic molecules to impressive accuracy. However, it remains to be seen whether the solvation free energies of macromolecules can be determined with similar accuracy.

Daranas et al. showed that the absence of reliable solvation thermodynamic data on proteins and protein–ligand complexes can be overcome in large part by considering the *relative* thermodynamics of association between closely related ligands binding to the same protein [23]. In this method knowledge of the solvation contribution from the free protein and from the protein–ligand complex is not required. The basis of the method involves a "three-dimensional" Born–Haber cycle as illustrated in Fig. 6, where P represents a given protein and $L1$ and $L2$ represent two closely related ligands. Since H is a state function, we can write:

$$\Delta H^{\circ}_{\mathrm{obs2}} - \Delta H^{\circ}_{\mathrm{obs1}} = \left[\Delta H^{\circ}_{i2} - \Delta H^{\circ}_{i1}\right] + \left\{\left[\Delta H^{\circ}_{\mathrm{sb2}} - \Delta H^{\circ}_{\mathrm{sb1}}\right] - \left[\Delta H^{\circ}_{\mathrm{su2}} - \Delta H^{\circ}_{\mathrm{su1}}\right]\right\} , \tag{17}$$

where the various terms are defined by analogy with Eqs. 11 and 12. The second of the solvation terms in curly braces represents the difference between the standard solvation enthalpies of the species prior to association, and since each ligand binds to the same protein, the solvation term for the free protein cancels. The first term in curly braces represents the difference between the solvation enthalpies of the complexes. If the same number and location of water molecules exists in the two complexes, then this term also cancels to first order. Thus, Eq. 17 simplifies to:

$$\Delta H^{\circ}_{\mathrm{obs2}} - \Delta H^{\circ}_{\mathrm{obs1}} = \left[\Delta H^{\circ}_{i2} - \Delta H^{\circ}_{i1}\right] - \left\{\left[\Delta H^{\circ}_{\mathrm{sl2}} - \Delta H^{\circ}_{\mathrm{sl1}}\right]\right\} , \tag{18}$$

where $\Delta H^{\circ}_{\mathrm{sl1}}$ and $\Delta H^{\circ}_{\mathrm{sl2}}$ are the standard solvation enthalpies of the ligands prior to association. Thus, provided that there are no structural changes in the protein in binding either ligand (which is most likely to be satisfied if the ligands are very similar), it is possible to obtain a value for difference between the intrinsic standard enthalpies of binding of each ligand from the observed standard enthalpies of binding and the standard solvation enthalpies of the relevant ligand. Clearly, intrinsic free energies and enthalpies of binding can also be obtained if the equivalent parameters are available.

An alternative approach for the experimental determination of the solvent contribution to the enthalpy of binding that does not require explicit knowledge of solvation terms, involves solvent isotope substitution methods introduced by Chervenak and Toone [39]. This method can be understood

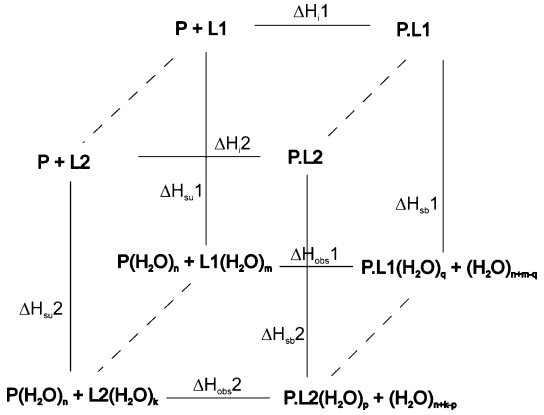

Fig. 6 "Three-dimensional" Born–Haber cycle for two ligands *L*1 and *L*2 binding to a given protein *P*, showing the relationship between the observed enthalpy of binding ΔH_{obs}, the "intrinsic" (solute–solute) enthalpy of binding ΔH_{i} and the solvation enthalpies of the unbound (ΔH_{su}) and bound $\left(\Delta H_{\mathrm{sb}}\right)$ species

in terms of a formalism devised by Muller to account for the solvation properties of a solute in a bath of *N* solvent water molecules. In this formalism, the enthalpy of solvation of the solute under these circumstances is described by:

$$\Delta H_{\mathrm{s}} = n^{\mathrm{h}} \left[\left(1 - f_{\mathrm{b}}\right) \Delta H_{\mathrm{b}}^{\mathrm{o}} - \left(1 - f_{\mathrm{hs}}\right) \Delta H_{\mathrm{hs}}^{\mathrm{o}} \right] . \tag{19}$$

This equation essentially describes the solvation enthalpy in terms of an enthalpic contribution from both bulk water ($\Delta H_{\mathrm{b}}^{\mathrm{o}}$) and from water in a "hydration shell" around the solute ($\Delta H_{\mathrm{hs}}^{\mathrm{o}}$). The fraction of broken hydrogen bonds in bulk solution is denoted f_{b}, with f_{hs} representing the analogous quantity for the hydration shell. The number of hydrogen bonds in the hydration shell is denoted n^{k}, and Muller suggested that a plausible value for this parameter is $3N/2$, since for a given N this is the largest geometrically allowed number of bonds between neighbouring molecules within the same shell. Isotopic substitution of D_2O for H_2O affects f_{b} differently from f_{hs} and $\Delta H_{\mathrm{b}}^{\mathrm{o}}$ from $\Delta H_{\mathrm{hs}}^{\mathrm{o}}$, due to the lower zero-point energy of deuterium with respect to protium. In contrast, the enthalpy of binding derived solely from solute–solute interactions (ΔH_i^{o}) will be unaffected by isotopic substitution providing the same number of hydrogen bonds exist in both solvents, i.e. the structures of the individual species prior to the association and the complex are identical in H_2O and D_2O. Thus, the determination of thermodynamic binding parameters using, for example, isothermal titration calorimetry (ITC) enables the crucial separation of intrinsic versus solvation terms. In the original application of this work [39], the authors concluded "that 25–100% of the net measured enthalpy of binding is accounted for by solvent reorganization".

An interesting application of the solvent isotopic substitution methods has been described by Connelly et al. [40] on the binding of the macrocycles FK506 and rapamycin to the FK506 binding protein. A feature of this protein–ligand complex is a hydrogen bond between a binding-site tyrosine in FK506 (Tyr-82 Hζ) and the ligand. In a Y82F mutant of FK506, Connelly et al. recorded a significantly more favourable binding enthalpy to FK506 and rapamycin compared with the wild-type protein ($\Delta\Delta H^{o}$ = – 17.6 and – 12.7 kJ/mol respectively). Moreover, significantly less favourable binding enthalpies were recorded on substitution of H_2O with D_2O for the Y82F mutant ($\Delta\Delta H^{o}$ = 18.0 and 12.1 kJ/mol for FK506 and rapamycin, respectively). These observations were rationalized by noting that the crystal structure of the unliganded protein shows two solvent water molecules ordered around the Tyr-82 hydroxyl group. The more favourable binding enthalpy in the Y82F mutant was suggested to arise from the desolvation of the latter group which was considered to be a highly unfavourable enthalpic process.

3.3 Entropic Contributions to Binding

3.3.1 Intrinsic Contribution

Intrinsic contributions to the entropy of binding arise from differences in dynamics between the free and bound states of both binding partners.

Considering first the ligand, the translational and rotational degrees of freedom that exist prior to the association will be lost on binding, giving rise to an unfavourable entropy term. Of course, the protein also possesses translational and rotational entropy, but since the magnitude of this entropy varies with the logarithm of particle mass, the loss in entropy on binding is approximately equivalent to the translational and rotational entropy of the smaller particle. If all of the translational and rotational motion is removed on binding, then the entropic cost of association is approximately + 57 kJ/mol for a small ligand [41]. However, in typical ligand-protein complexes, the noncovalent interaction energies are comparable to the thermal energies at physiological temperature and hence a degree of motion of the ligand exists in the binding site. The degree of such motion is extremely difficult to determine experimentally, and accordingly estimates of the translational and rotational contribution to the overall entropy of binding varies enormously (see e.g. Table 6 in Burkhalter et al. [24]) and has been estimated to be as low as + 5.4 kJ/mol [42].

In addition to the loss of translational and rotational motion, internal degrees of freedom of the ligand will typically be restricted on binding. In particular, torsional degrees of freedom are typically substantially attenuated

on binding. The entropy corresponding to internal rotation of a symmetric, free rotor (i.e. where any barrier to rotation is much less than kT) such as a methyl group can be calculated from the respective partition function which is given by:

$$Q_{\text{free}} = \left(\sigma_{\text{int}} h\right)^{-1} \left(8\pi^3 I_{\text{int}} kT\right)^{1/2} , \tag{20}$$

where σ_{int}, the internal symmetry number, is equal to the number of minima or maxima in the torsional potential, and I_{int} is the reduced moment of inertia for the internal rotation. The torsional entropy is given by:

$$S_{\text{free}} = R\left(0.5 + \ln Q\right) . \tag{21}$$

If the torsional barrier is comparable to kT (hindered rotor), then the torsional entropy is reduced by a factor that can be determined from tables compiled by Pitzer and Gwinn [43]. Typical values for the torsional entropy of hindered rotors such as a hydroxyl group or a hydroxymethyl group are 4.5 kJ/mol and 7.3 kJ/mol respectively. Once again, it is very difficult to determine experimentally the residual torsional motion that exists within a given ligand upon association, and consequently estimates of the contribution to the entropy of binding resulting from "freezing" of torsional degrees of freedom vary considerably. The entropy of fusion within homologous series of hydrocarbons provides an estimate of this entropic cost as – 1.6 to – 3.6 kJ/mol at 300 K within a hydrocarbon chain [44], suggesting that substantial torsional freedom is retained in the bound-state.

Turning now to the protein, restriction of degrees of freedom is also anticipated to occur upon ligand binding. A number of investigations have been reported within the last decade whereby protein dynamics has been correlated with binding thermodynamics using NMR relaxation techniques [45–54]. Since each resonance in an NMR spectrum corresponds to an individual nucleus or group of equivalent nuclei, relaxation measurements offer the potential to obtain thermodynamic parameters at discrete sites within a macromolecule. The details of such measurements are outside the scope of this work, and the reader is referred to several excellent reviews [55–64]. Essentially, the time decay of nuclear magnetization is determined as a function of time, from which characteristic relaxation rates can be determined. These can in turn be interpreted in terms of a formalism for the dynamic motions to which these relaxation rates are sensitive [65], giving rise to a generalized order parameter S that defines the extent of internal motions on the ps–ns timescale.

Early work by Akke et al. [45] described the derivation of free energies of binding from differences in the square of the NMR-derived generalized order parameter S^2 [65] determined from backbone ^{15}N relaxation data for calbindin in the "apo" and ligand (Ca^{2+}) bound states. In an important further advance, Li et al. [66] used a simple one-dimensional vibrator as a model for

dynamic motion to illustrate the relationship between dynamics measured by NMR relaxation methods and the local residual entropy of proteins. They concluded that dynamics of methyl containing side-chains in proteins corresponds to a substantial entropic contribution to the free energy of ubiquitin of approximately 40 kcal/mol at 300 K. Subsequently, Yang and Kay [46, 67] examined the relation between the order parameter and conformational entropy from ns–ps bond vector dynamics considering a number of simple models describing bond vector motion. Although it was not possible to derive equations relating the order parameter to conformational entropy for the majority of models considered, an approximate relation was found to describe order parameters vs. entropy profiles extremely well:

$$S_p/k = A + \ln \pi \left[3 - (1 + 8S)^{1/2}\right] , \tag{22}$$

where A is a model-dependent constant.

The studies above suggest that the measurement of both the free energy and entropy of binding for a biomolecular association is possible on a per-residue basis. Moreover, the enthalpy of binding could thus be determined from Eq. 1. Unfortunately, however, as discussed by Yang and Kay [46], the free energy change between states derived from this approach, unlike the entropy change, is dependent upon differences in ground state energies. Since the latter are in general unavailable, NMR relaxation measurements are only able to offer reliable insight into the entropy of binding. There is a number of assumptions in the derivation of Eq. 22 [46, 56]. First, this equation contains the model dependent constant A, and in general the nature of the motional model is unknown. In the case of the entropy of binding this is not a severe limitation if the assumption is made that the motional models before and after association are similar, in which case the constant A cancels. Second, the order parameter measured from conventional heteronuclear relaxation measurements is sensitive only to motions on a time scale shorter than overall rotational diffusion (picoseconds to nanoseconds), and is sensitive only to reorientational motions of the relevant bond vector. Third, no account is taken of correlated motions between different bond vectors. However, despite these limitations, NMR relaxation measurements can provide reasonably accurate per-residue entropies for a variety of biomolecular associations (vide infra).

Backbone dynamics of proteins are typically probed by detecting the reorientation of the amide bond vector in ^{15}N-enriched proteins. Conformational entropies of NH groups for each amino-acid residue can be measured from ^{15}N relaxation data assuming a diffusion-in-a-cone model for NH vector motions [46]. In the case of side-chain dynamics measurements, the nucleus of choice is deuterium. The reasons for this choice are discussed at length elsewhere [68–70]. More recently, Millet et al. [71] have described an approach whereby five relaxation rates per deuteron can be obtained in ^{13}C-labelled and fractionally ^{2}H-enriched proteins, enabling self-consistency of the relaxation data to be established.

One of the first applications of the above approach considered the conformational entropy change associated with the folding-unfolding transition in the N-terminal SH3 domain of the Drosophila signal transduction protein drk [46]. The observed entropy change for the folding-unfolding transition averaged 12 J/mol K, compared with the average entropy change per residue estimated from alternative techniques of $\sim$ 14 J/mol K [72]. In a subsequent study, Wrabl et al. [73] used simulated order parameters for N – H bond vectors from nanosecond molecular dynamics simulations of staphylococcal nuclease, and compared per-residue entropies calculated using Eq. 4 with those estimated using quasiharmonic analysis [74]. A positive correlation between these parameters suggested that NMR-derived order parameters provide a reasonable estimate of the total conformational entropy change on protein folding.

A number of studies using NMR relaxation methods have shown that changes in the conformational entropy of the protein before and after ligand association can make significant contributions to the free energy of binding. For example, Bracken et al. [48] examined the dynamics of the leucine zipper domain of yeast transcription factor GCN4 on binding to DNA. In the absence of DNA, the N-terminal basic region adopts an ensemble of transient structures, but undergoes a transition to yield a stable α-helical structure on binding DNA. Thus, an unfavourable contribution to binding is anticipated from the change in conformational entropy of the protein backbone, which was estimated as – 0.6 kJ/mol/K, which agrees remarkably well with theoretical predictions based on calorimetric measurements for the same system (– 0.5 kJ/mol/K). At 300 K the contribution to the free energy of binding is thus between – 150 and – 180 kJ/mol. This contribution is likely offset by a number of other competing factors described in this section, but it illustrates that the unfavourable entropic contribution from freezing protein degrees of freedom on binding can be very significant.

Lee et al. examined the entropic contribution to binding from both backbone and side-chain degrees of freedom for calcium saturated calmodulin binding with a peptide model of the calmodulin-binding domain of myosin light chain kinase [52]. A remarkable result of these studies is that the protein effectively redistributes the side-chain entropy upon binding of the peptide. The side-chains of binding-site residues become more rigid upon association of the peptide as anticipated, whereas certain residues remote from the binding site become more flexible, thus offsetting in part the unfavourable entropic contribution from binding-site residues. Once again, the overall entropic contribution to binding free energy derived from NMR relaxation measurements is in qualitative agreement with calorimetric measurements.

More recently Bingham et al. [54] undertook a study of the binding of 2-methoxy-3-isobutylpyrazine (IBMP) and 2-methoxy-3-isopropylpyrazine (IPMP) to the major urinary protein. Backbone dynamics of certain regions of the protein exhibited increased flexibility on binding either lig-

and, whereas others displayed an overall reduction in flexibility (Fig. 7). The overall entropic contribution from backbone dynamics was unfavourable with $T\Delta S = -7.4 \pm 6.5$ kJ/mol. The overall contribution from side-chain methyl dynamics on binding IBMP was also unfavourable ($T\Delta S_b = -3.4 \pm 2.8$ kJ/mol), and in common with the calmodulin-peptide complex studied by Lee et al. [52], "entropy–entropy compensation" is observed, i.e. loss of dynamics for binding-site residues is offset by increased dynamics of side chains distal to the binding site.

The NMR measurements discussed thus far in this section probe dynamics on the ps–ns timescale. Dynamic changes on binding over timescales outside this regime, such as slower motions resulting from domain motions or substantial conformational rearrangement, will also clearly contribute to the entropy of binding. The internal motions that give rise to such phenomena typically have time constants in the microsecond to millisecond range, and the relaxation times $T_1\rho$ and T_2 are very sensitive to these motions since they contribute to resonance line-widths. Under the appropriate circumstances, relaxation dispersion experiments can be utilized to extract kinetic and thermodynamic parameters and chemical shift differences between the interconverting states [58, 75–85]. Experiments that have been most recently developed monitor transverse ^{15}N or ^{13}C relaxation during Carr-Purcell-Meiboom-Gill (CPMG) pulse trains [86], with effective relaxation rates measured as a function of the average CPMG radio frequency field strength. Loosely, the function of the CPMG pulse train can be thought of as suppressing chemical shift information, the extent of which depends on the applied CPMG field strength. At low field strengths, transverse relaxation rates are larger due to the presence of a contribution from conformational exchange. Conversely, at large field strengths, the exchange contribution is

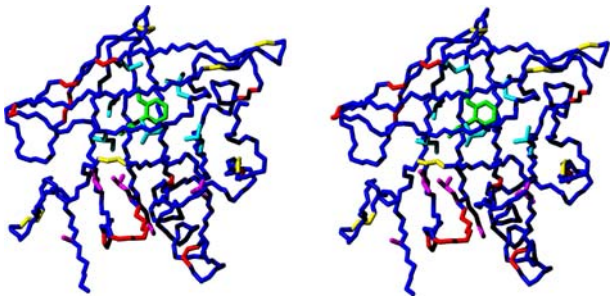

Fig. 7 Structural details of residues that contribute to the entropy of binding of 2-methoxy-3-isobutylpyrazine to MUP-I. Backbone residues that exhibit an unfavourable entropic contribution to binding are *coloured yellow*, while those that exhibit a favourable contribution are *coloured red*. Similarly, residues whose methyl-containing sidechains exhibit an unfavourable contribution are *coloured light blue*, whereas those that exhibit a favourable contribution are *coloured magenta*. Reproduced with permission from J Am Chem Soc 2004, 126:1675–1681. Copyright 2004 Am Chem Soc

largely suppressed, since it depends, inter alia, upon the chemical shift difference between exchanging sites.

Yung et al. recently applied the relaxation dispersion technique to probe the influence of conformational exchange in the homopentameric B subunit (VTB) of the toxin from E. coli O157 on the thermodynamics of binding of a novel ligand known as "Pk dimer" [87]. VTB is known to possess three binding sites for the natural carbohydrate ligand globotriaosylceramide on each monomeric subunit [88]. Kitov et al. designed the potential chemotherapeutic agent Pk dimer to straddle two adjacent binding sites, in order to optimize binding affinity through multivalency [89]. Remarkably, the binding of this ligand to the B subunit gives rise to a narrowing of the line-width of a number of resonances in the $^{15}N - ^{1}H$ heteronuclear single quantum correlation (HSQC) of the protein (Fig. 8). This is at first sight counter-intuitive since linewidths are generally expected to increase due to the larger rotational tumbling time of the complex. However, this phenomenon can be explained by the presence of conformational exchange in the homopentamer before complexation that is suppressed on ligand binding. Interestingly, an early crystal structure of VTB in the absence of ligand showed an asymmetric structure for the protein, where two adjacent monomers were displaced giving the appearance of a "lockwasher" [90]. In contrast, the NMR-derived average structure suggested a symmetric homopentamer [91]. Typical relaxation dispersion profiles for VTB are shown in Fig. 9. Notably, residues that displayed the most significant relaxation dispersion were located at the monomer-monomer interface. These data were qualitatively consistent with interconversion between the symmetric, lower energy state, and a higher energy state that might be related to that observed in the crystal structure. Quantitatively, relaxation dispersion profiles can be fit to suitable expressions for the exchange process. In the limit of fast exchange between two sites the relevant expression is [92]:

$$R_2\left(\nu_{\mathrm{CPMG}}\right) = R_2\left(\nu_{\mathrm{CPMG}} = \infty\right) + \left(p_{\mathrm{a}} p_{\mathrm{b}} \delta\omega^2 / k_{\mathrm{ex}}\right) \times \left(1 - \left(4\nu_{\mathrm{CPMG}}/k_{\mathrm{ex}}\right) \tanh\left(k_{\mathrm{ex}}/4\nu_{\mathrm{CPMG}}\right)\right) , \quad (23)$$

where ν_{CPMG} is the CPMG field strength, p_{a} and p_{b} are the populations of states a and b, and k_{ex} is the exchange rate. Fitting of relaxation dispersion profiles in Fig. 9 to Eq. 23 gave rise to a single effective value of k_{ex} over a number of sites, indicating that a concerted exchange process was taking place at the monomer-monomer interface. Relaxation dispersion was unobservable in the presence of the ligand, which straddles adjacent monomers and effectively quenches the conformational exchange. Correspondingly, binding curves for the titration of Pk dimer with VTB probed using either ^{15}N chemical shift perturbations or ITC experiments could not be fitted to a simple two-state binding model. However, these data could be well-fitted with a co-operative sequential binding model. Assuming that a sec-

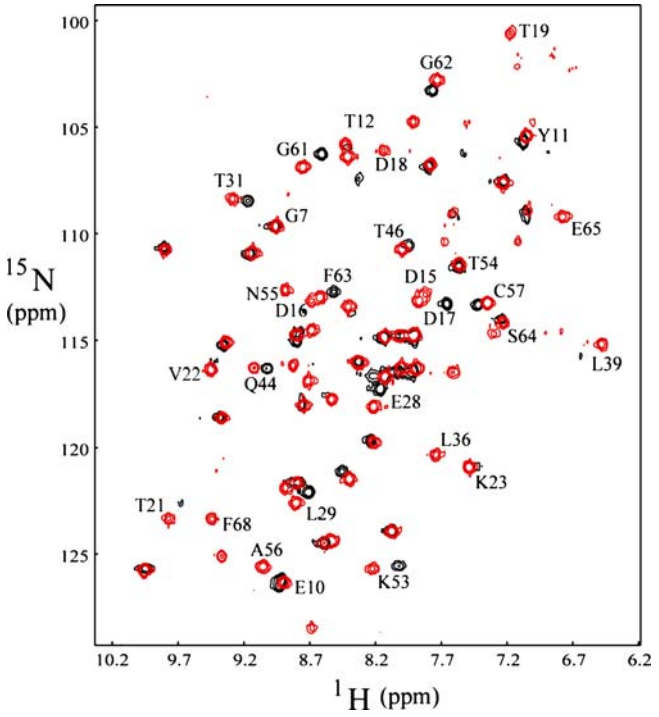

Fig. 8 $^{15}N-{}^{1}H$ HSQC spectra of VTB in the absence (*black contours*) and presence (*red contours*) of bivalent inhibitor Pk-dimer. Resonance assignments of residues that experience a shift on inhibitor binding are labelled. Note that in a number of instances (e.g. L39 to the *right of the figure*) the resonance is broadened to the limit of, or below detection in the absence of inhibitor. Reproduced with permission from J Am Chem Soc 2003, 125:13058–13062. Copyright 2003 Am Chem Soc

ond Pk-dimer molecule bound to the homopentamer does not interact with the first, the entropic cost of suppressing conformational exchange by the first binding event was estimated to be – 68.5 kJ/mol at 45 °C. Thus, it is clear that conformational rearrangement can give rise to a very significant unfavourable entropic contribution to binding.

A conceptually different approach for characterizing protein dynamics involves the measurement of three-bond scalar couplings, which can report on rotamer distributions of amino-acid sidechains [93–95]. No information on the timescale of such motions is available from these measurements, but importantly scalar couplings are sensitive to motions over the entire range from picoseconds to milliseconds. Chou et al. [96] measured $^{3}J_{C'-C\gamma}$ and $^{3}J_{N-C\gamma}$ scalar couplings to determine the degree of side-chain order about the C^{α}–C^{β} bond ($\chi 1$ angle) for threonine, isoleucine and valine residue sidechains in ubiquitin. By use of the relevant Karplus parametrization, rotamer populations could be derived from a which a generalized order parameter, S_{J}^{2}, was

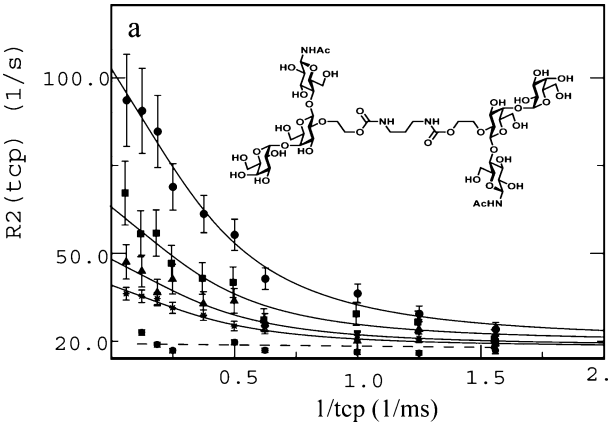

Fig. 9 Typical ^{15}N relaxation dispersion profiles for the amide nitrogens of Val 50 (●), Val 22 (■), and Lys 23 (▲) in VTB. The relaxation dispersion profile for Val 50 in the presence of 5-fold molar excess of inhibitor Pk-dimer (*inset*) is shown by the *broken line*. *Solid lines* represent the best-fit to the data using the equation appropriate for all exchange time-scales with $k_{ex} = 1000\,s^{-1}$. Reproduced with permission from J Am Chem Soc 2003, 125:13058–13062. Copyright 2003 Am Chem Soc

calculated according to the following expression:

$$S_J^2 = \sum_{i,j} P_i P_j \left(3\cos^2\theta_{ij} - 1\right)/2\,, \tag{24}$$

where the summation is over all pairwise combinations of the three rotamers, P_i is the population of rotamer i and θ_{ij} is the angle between the $C^\beta - C^\alpha$ bond vectors of rotamers i and j. Comparison of the order parameters thus obtained with those derived from methyl ^{2}H relaxation rates for the same residues gave a correlation coefficient of 0.81, which is remarkable given that the two approaches measure the order parameters over very different time-scales. To the knowledge of the author scalar coupling measurements have not been used to probe the contribution of side-chain motions to binding entropy, but clearly these are highly complementary to relaxation methods for this purpose.

3.3.2 Solvation Contribution

Entropies of solvation of small organic ligands are typically negative [25, 97]. This makes intuitive sense given the proposed solvent ordering around the solute in the current view of the hydrophobic effect (Sect. 2.2). To the extent that ligand binding is a desolvation process, it is therefore anticipated that solvent reorganization will offer a favourable entropic contribution to binding. The magnitude of this contribution has been a topic of considerable

debate. As described by Dunitz, there are however limits for the entropic cost of bound water in biomolecules [98]. Comparison of the standard entropies at 298 K for anhydrous and hydrated inorganic salts shows that a bound water molecule in crystalline hydrates contributes approximately 42 J/mol/K to the standard entropy. Since the standard entropy at 298 K of liquid water is approximately 70 J/mol/K, the entropic cost of immobilizing a given water molecule in a crystalline lattice is thus approximately – 28 J/mol/K. Since a water molecule within the solvation cage of a nonpolar ligand or a protein binding site will not be bound more firmly than a crystalline hydrate, this value can be taken as the maximum entropic cost of ordering, which corresponds to a standard free energy of approximately 8.3 kJ/mol at 298 K. Thus, the release of a solvent water molecule from the solvation shell of a ligand or from a protein binding-site on binding is anticipated to correspond to a maximum – 8.3 kJ/mol favourable contribution to the free energy of binding.

Direct experimental measurement of the entropic contribution from bound water molecules in fraught with difficulty, and most conclusions have arisen from indirect observations. An interesting example is the study of Holdgate et al. [99] on the binding of the antibiotic novobiocin to a resistant mutant of DNA gyrase. Novobiocin binds to a 24 kDa fragment from the B subunit of DNA gyrase, and resistance to this antibiotic occurs from mutation of Arg-136 which hydrogen bonds to the coumarin ring of novobiocin. Holdgate et al. showed that an R136H mutant binds with a K_d that increases from 32 nM to 1200 nM compared with the wild-type protein at 300 K. This increased affinity was shown by isothermal titration calorimetry measurements to arise from a more favourable enthalpy of binding and a much less favourable entropy of binding. This is opposite to the expected thermodynamic signature given that the loss of the arginine residue is expected to reduce solute–solute hydrogen bonding. However, in the crystal structure of the mutant complex, an ordered water molecule is sequestered into the region vacated by the arginine guanidinium group. Holdgate et al. suggested that the resulting water-mediated protein-antibiotic hydrogen bonds give rise to a favourable enthalpic contribution, whereas the sequestration of a water molecule leads to an entropic cost and reduction in heat capacity of the system.

Further experimental evidence for an entropic contribution to binding derives from the work of Clarke et al. [100] on the binding of trimannoside oligosaccharides to the plant lectin concanavalin A (Con A). These authors characterized the thermodynamics of binding of Manα1-6(Manα1-3)Manα1-OMe and a derivative bearing a hydroxyethyl moiety at C-2 of the central mannose unit to Con A using ITC. Molecular dynamics simulations of the complexes of Con A with each of these ligands established that the hydroxyethyl moiety displaces a conserved water molecule present in the Con A binding site. Correspondingly, the binding of the hydroxyethyl derivative displayed a more favourable entropy and a relatively large unfavourable enthalpy

term in comparison with the underivatized ligand. It was proposed that an indirect interaction through the water molecule in the complex with the latter provides a larger number of hydrogen bonds in the complex that have higher occupancies than in bulk solution, thus providing enthalpic stabilization. The more favourable entropy of binding of the hydroxyethyl derivative was suggested to derive from expulsion of the conserved water molecule that is present in the uncomplexed protein into bulk solvent.

The above studies probed the entropic contribution to binding from the solvent *indirectly* via changes in the thermodynamic signature of binding. It is very difficult experimentally to probe *directly* the entropic contribution to binding from the solvent. X-ray diffraction data often show bound water molecules in protein binding sites, but only if these are well-ordered and the occupancy is sufficiently high. Moreover, NMR methods typically report on the average properties of solvent water molecules, and since exchange with bulk solvent is typically fast on the NMR time-scale, it is difficult although not impossible [101] to observe ordered water molecules, but the extraction of accurate thermodynamic parameters is a different matter. Despite these difficulties, pioneering work by Halle and coworkers using ^{17}O, ^{2}H and ^{1}H NMR dispersion measurements has made significant progress in this direction [102, 103]. In principle, relaxation dispersion measurements on solvent water are similar to those described in Sect. 3.3.1. However, the exchange rates for solvent water molecules transiently bound to proteins are much greater than rates of conformational change within proteins, and it is necessary to vary the static magnetic field rather than a weak spin-locking field in order to record water relaxation dispersion profiles. Such measurements have however shown that the three buried water molecules in bovine pancreatic trypsin inhibitor exchange with bulk water on a time-scale of 15 ns to 1 μs and undergo librational motions of considerable amplitude in proteins [104]. Analysis of three independent order parameters provided by relaxation dispersion data for ^{17}O, ^{2}H and ^{1}H in terms of an anisotropic harmonic libration model, provided the amplitude and anisotropy of water rotation within the protein. Although each of the buried water molecules investigated engage in three or four hydrogen bonds, entropies were found to span the range from ice to bulk water, suggesting that the hydration of cavities in proteins with weaker hydrogen-bonding capacity may be entropically driven. Thus, these data contradict the conventional view (described in the previous two paragraphs) that ligand binding to proteins is entropically favored by release of ordered water.

Further insight into the entropic contribution of solvent water molecules has been obtained from atomistic molecular dynamics simulations. Li and Lazaridis used inhomogeneous fluid solvation theory to study the contribution of a bound water molecule in the binding site of HIV-1 protease to the energy, entropy and heat capacity of solvation [105]. The entropy loss in binding this water molecule was found to be 41 J mol^{-1} K^{-1} and the total contribution

to the free energy of solvation was found to be – 63.5 kJ mol^{-1}. Notably, the calculated entropy is significantly larger than that predicted by Dunitz [98]. Hamelberg and McCammon, using rigorous statistical mechanical molecular dynamics simulations, computed the standard free energy of releasing a bound water molecule from the binding pocket in a Trypsin/Benzylamine complex and an HIV-1/KNI-272 complex [106]. Values of $\sim$ – 8 kJ mol^{-1} and – 13 kJ mol^{-1} respectively, were obtained, suggesting that localized water molecules stabilize ligand-protein interactions in both complexes.

4 Concluding Remarks

Complete dissection of the thermodynamics of binding of a ligand to a protein into enthalpic and entropic contributions from both partners and the solvent is a formidable task. However, it is a battle that must ultimately be won in order to make use of the rapidly increasing numbers of high-resolution protein structures in "rational" drug design. Although much remains to be done, significant progress has been made in the last decade. For example, high-resolution NMR methods have shed light on the contribution of protein degrees of freedom to the entropy of binding on a *per-residue* basis for a number of systems. While the approach is subject to a number of assumptions, a feature of the binding process in systems studied to date is the reduction in the unfavourable entropic contribution to binding resulting from freezing of binding site residues by melting of binding site residues at distal locations. This entropy–entropy compensation phenomenon may be a universal property of proteins. At present we know insufficient detail about protein dynamics to predict this phenomenon, and hence it will be difficult to exploit it for rational ligand design purposes. It is tempting to speculate that mutations distal to binding-site regions in various protein drug targets in resistant bacterial strains may derive from dynamic processes such as these, although this has not been examined experimentally to our knowledge. Turning to the enthalpy of binding, the notion of binding-site "shape" complementarity has long been a mainstay of computational approaches to lead compound design. The recent discovery that solute–solvent van der Waals interactions do not necessarily exchange for solute–solute van der Waals interactions in protein binding sites that are sub-optimally hydrated [107], offers the possibility to obtain dramatic increases in the free energy of binding by optimizing shape complementarity in such systems. Whether this approach is worthwhile will clearly be dependent on the degree of hydration of the binding pocket, which to our knowledge has not been systematically examined.

Despite these advances, there are still many gaps in our knowledge. Perhaps the most contentious area concerns the thermodynamic contribution from solvent water. For every "quantitative" measure of the enthalpic and en-

tropic contribution from, for example, bound water molecules, it appears that there are conflicting data. The only common feature appears to be that the thermodynamic contribution from solvent water can be significant. There is general agreement that the ejection of bound water molecules from a binding pocket into bulk solvent on ligand binding is an entropically favourable process, but the enthalpic contribution from this process remains a matter for debate. Resolution of these issues is likely to be extremely difficult. NMR methods, except in certain special cases, only provide information on the average properties of solvent water molecules, which typically exchange rapidly between the protein-bound state and bulk water. X-ray diffraction methods can only detect bound water molecules if the occupancy or degree of order is sufficiently high. All atom molecular dynamics simulations perhaps provide the greatest hope of quantifying the solvation contribution, but the current level of accuracy of molecular mechanical forcefields leaves some concerns regarding the validity of the data thus obtained.

References

1. Frank HS, Evans MW (1945) J Chem Phys 13:507
2. Nemethy G, Scheraga HA (1962) J Chem Phys 36:3382
3. Tanford C (1980) The Hydrophobic Effect: Formation of Micelles and Biological Membranes. Wiley, New York
4. Privalov PL, Gill SJ (1988) Adv Protein Chem 39:191
5. Mirejovsky D, Arnett EM (1983) J Am Chem Soc 105:1112
6. Lee SH, Rossky PJ (1994) J Chem Phys 100:3334
7. Lee B (1991) Biopolymers 31:993
8. Lee B (1985) Biopolymers 24:813
9. Lucas M (1976) J Phys Chem 80:359
10. Southall NT, Dill KA, Haymet ADJ (2002) J Phys Chem B 106:521
11. Southall NT, Dill KA (2002) Biophys Chem 101:295
12. Chandler D (2005) Nature 437:640
13. Williams DH, Bardsley B (1999) Perspect Drug Discov Design 17:43
14. Wiseman T, Williston S, Brandts JF, Lin LN (1989) Anal Biochem 179:131
15. Penel S, Doig AJ (2001) J Mol Biol 305:961
16. Williams DH, Stephens E, Zhou M (2003) J Mol Biol 329:389
17. Hyre DE, Le Trong I, Freitag S, Stenkamp RE, Stayton PS (2000) Prot Sci 9:878
18. Vondrasek J, Bendova L, Klusak V, Hobza P (2005) J Am Chem Soc 127:2615
19. Ross PD, Subramanian S (1981) Biochemistry 20:3096
20. Chapman KT, Still WC (1989) J Am Chem Soc 111:3075
21. Hunter CA (2004) Angew Chem Int Ed 43:5310
22. Talhout R, Villa A, Mark AE, Engberts J (2003) J Am Chem Soc 125:10570
23. Daranas AH, Shimizu H, Homans SW (2004) J Am Chem Soc 126:11870
24. Burkhalter NF, Dimick SM, Toone EJ (2000) In: Ernst B, Hart GW, Sinay P (eds) Carbohydrates in Chemistry and Biology. Part I: Chemistry of Saccharides, Vol 2. Wiley, Weinheim, p 863
25. Cabani S, Gianni P, Mollica V, Lepori L (1981) J Sol Chem 10:563

26. Plyasunov AV, Shock EL (2000) Geochim Cosmochim Acta 64:439
27. Muller N (1990) Acc Chem Res 23:23
28. Buttery RG, Bomben JL, Guadagni DG, Ling LC (1971) J Agric Food Chem 19:1045
29. Orozco M, Luque FJ (2000) Chem Rev 100:4187
30. Kollman PA (1993) Chem Rev 93:2395
31. Carlson HA, Nguyen TB, Orozco M, Jorgensen WL (1993) J Comput Chem 14:1240
32. Orozco M, Jorgensen WL, Luque FJ (1993) J Comput Chem 14:1498
33. Jorgensen WL, Nguyen TB (1993) J Comput Chem 14:195
34. Wan S, Stote RH, Karplus M (2004) J Chem Phys 121:9539
35. Kubo MM, Gallicchio E, Levy RM (1997) J Phys Chem B 101:10527
36. Chothia C (1974) Nature 248:338
37. Levy RM, Zhang LY, Gallicchio E, Felts AK (2003) J Am Chem Soc 125:9523
38. Hawkins GD, Cramer CJ, Truhlar DG (1997) J Phys Chem B 101:7147
39. Chervenak MC, Toone EJ (1994) J Am Chem Soc 116:10533
40. Connelly P, Aldape RA, Bruzzese FJ, Chambers SP, Fitzgibbon MJ, Fleming MA, Itoh S, Livingston DJ, Navia MA, Thomson JA, Wilson KP (1994) Proc Natl Acad Sci 91:1964
41. Jencks WP (1981) Proc Natl Acad Sci 78:4046
42. Williams DH, Stephens E, O'Brien DP, Zhou M (2004) Angew Chem Int Ed 43:6596
43. Pitzer KS, Gwinn WD (1942) J Chem Phys 10:428
44. Searle MS, Williams DH (1992) J Am Chem Soc 114:10690
45. Akke M, Bruschweiler R, Palmer AG (1993) J Am Chem Soc 115:9832
46. Yang DW, Kay LE (1996) J Mol Biol 263:369
47. Spyracopoulos L, Gagne SM, Li MX, Sykes BD (1998) Biochemistry 37:18032
48. Bracken C, Carr PA, Cavanagh J, Palmer AG (1999) J Mol Biol 285:2133
49. Zídek L, Novotny MV, Stone MJ (1999) Nature Str Biol 6:1118
50. Sahu SC, Bhuyan AK, Udgaonkar JB, Hosur RV (2000) J Biomol NMR 18:107
51. Maler L, Blankenship J, Rance M, Chazin WJ (2000) Nature Str Biol 7:245
52. Lee AL, Kinnear SA, Wand AJ (2000) Nature Str Biol 7:72
53. Loh AP, Pawley N, Nicholson LK, Oswald RE (2001) Biochemistry 40:4590
54. Bingham R, Bodenhausen G, Findlay JHBC, Hsieh S-Y, Kalverda AP, Kjellberg A, Perazzolo C, Phillips SEV, Seshadri K, Turnbull WB, Homans SW (2004) J Am Chem Soc 126:1675
55. Palmer AG (1997) Curr Op Struct Biol 7:732
56. Cavanagh J, Akke M (2000) Nature Str Biol 7:11
57. Palmer AG (2001) Ann Rev Biophys 30:129
58. Palmer AG, Kroenke CD, Loria JP (2001) Meth Enzymol 339:204
59. Spyracopoulos L, Sykes BD (2001) Curr Op Struct Biol 11:555
60. Frueh D (2002) Progr NMR Spectrosc 41:305
61. Luginbuhl P, Wuthrich K (2002) Progr NMR Spectrosc 40:199
62. Case DA (2002) Acc Chem Res 35:325
63. Kempf JG, Loria JP (2003) Cell Biochem Biophys 37:187
64. Palmer AG (2004) Chem Rev 104:3623
65. Lipari G, Szabo A (1982) J Am Chem Soc 104:4546
66. Li ZG, Raychaudhuri S, Wand AJ (1996) Prot Sci 5:2647
67. Yang DW, Mok YK, FormanKay JD, Farrow NA, Kay LE (1997) J Mol Biol 272:790
68. Muhandiram DR, Yamazaki T, Sykes BD, Kay LE (1995) J Am Chem Soc 117:11536
69. Lee AL, Flynn PF, Wand AJ (1999) J Am Chem Soc 121:2891
70. Ishima R, Petkova AP, Louis JM, Torchia DA (2001) J Am Chem Soc 123:6164
71. Millet O, Muhandiram DR, Skrynnikov NR, Kay LE (2002) J Am Chem Soc 124:6439

72. Doig AJ, Sternberg MJE (1995) Prot Sci 4:2247
73. Wrabl JO, Shortle D, Woolf TB (2000) Proteins 38:123
74. Tidor B, Karplus M (1994) J Mol Biol 238:405
75. Millet O, Loria JP, Kroenke CD, Pons M, Palmer AG (2000) J Am Chem Soc 122:2867
76. Mulder FAA, van Tilborg PJA, Kaptein R, Boelens R (1999) J Biomol NMR 13:275
77. Akke M, Liu J, Cavanagh J, Erickson HP, Palmer AG (1998) Nature Str Biol 5:55
78. Davis DG, Perlman ME, London RE (1994) J Magn Reson B 104:266
79. Allerhand A, Gutowsky HS (1965) J Chem Phys 42:1587
80. Mulder FAA, Hon B, Muhandiram DR, Dahlquist FW, Kay LE (2000) Biochemistry 39:12614
81. Skrynnikov NR, Mulder FAA, Hon B, Dahlquist FW, Kay LE (2001) J Am Chem Soc 123:4556
82. Ishima R, Louis JM, Torchia DA (1999) J Am Chem Soc 121:11589
83. Ishima R, Torchia DA (1999) J Biomol NMR 14:369
84. Mulder FAA, Mittermaier A, Hon B, Dahlquist FW, Kay LE (2001) Nature Str Biol 8:932
85. Mulder FAA, Hon B, Mittermaier A, Dahlquist FW, Kay LE (2002) J Am Chem Soc 124:1443
86. Carr HY, Purcell EM (1954) Phys Rev 94:630
87. Yung A, Turnbull WB, Kalverda AP, Thompson GS, Homans SW, Kitov P, Bundle DR (2003) J Am Chem Soc 125:13058
88. Ling H, Boodhoo A, Hazes B, Cummings MD, Armstrong GD, Brunton JL, Read RJ (1998) Biochemistry 37:1777
89. Kitov PI, Shimizu H, Homans SW, Bundle DR (2003) J Am Chem Soc 125:3284
90. Stein PE, Boodhoo A, Tyrrell GJ, Brunton JL, Read RJ (1992) Nature 355:748
91. Richardson JM, Evans PD, Homans SW, DonohueRolfe A (1997) Nature Str Biol 4:190
92. Luz Z, Meiboom S (1963) J Chem Phys 39:366
93. Dzakula Z, Westler WM, Edison AS, Markley JL (1992) J Am Chem Soc 114:6195
94. Dzakula Z, Edison AS, Westler WM, Markley JL (1992) J Am Chem Soc 114:6200
95. Perez C, Lohr F, Ruterjans H, Schmidt JM (2001) J Am Chem Soc 123:7081
96. Chou JJ, Case DA, Bax A (2003) J Am Chem Soc 125:8959
97. Ben-Naim A, Marcus Y (1984) J Chem Phys 81:2016
98. Dunitz J (1994) Science 264:670
99. Holdgate GA, Tunnicliffe A, Ward WHJ, Weston SA, Rosenbrock G, Barth PT, Taylor IWF, Pauptit RA, Timms D (1997) Biochemistry 36:9663
100. Clarke C, Woods RJ, Gluska J, Cooper A, Nutley MA, Boons G-J (2001) J Am Chem Soc 123:12238
101. Otting G, Wuthrich K (1989) J Am Chem Soc 111:1871
102. Halle B, Andersson T, Forsen S, Lindman B (1981) J Am Chem Soc 103:500
103. Denisov VP, Halle B (1995) J Mol Biol 245:682
104. Denisov VP, Venu K, Peters J, Horlein HD, Halle B (1997) J Phys Chem B 101:9380
105. Li Z, Lazaridis T (2003) J Am Chem Soc 125:6636
106. Hamelberg D, McCammon JA (2004) J Am Chem Soc 126:7683
107. Barratt E, Bingham R, Warner DJ, Laughton CA, Phillips SEV, Homans SW (2005) J Am Chem Soc 127:11827